

Drell–Yan lepton-pair production: q_T resummation at N^4LL accuracyStefano Camarda ^a, Leandro Cieri ^b, Giancarlo Ferrera ^{c,*}^a CERN, CH-1211 Geneva, Switzerland^b Instituto de Física Corpuscular, Universitat de València - Consejo Superior de Investigaciones Científicas, Parc Científic, E-46980 Paterna, Valencia, Spain^c Dipartimento di Fisica, Università di Milano and INFN, Sezione di Milano, I-20133 Milan, Italy

ARTICLE INFO

Article history:

Received 14 April 2023

Received in revised form 26 July 2023

Accepted 10 August 2023

Available online 18 August 2023

Editor: B. Grinstein

ABSTRACT

We consider Drell–Yan lepton pairs produced in hadronic collisions. We present high-accuracy QCD predictions for the transverse-momentum (q_T) distribution and fiducial cross sections in the small q_T region. We resum to all perturbative orders the logarithmically enhanced contributions up to the next-to-next-to-next-to-leading logarithmic (N^4LL) accuracy and we include the hard-virtual coefficient at the next-to-next-to-next-to-leading order (N^3LO) (i.e. $\mathcal{O}(\alpha_S^3)$) with an approximation of the N^4LO coefficients. The massive axial-vector and vector contributions up to three loops have also been consistently included. The resummed partonic cross section is convoluted with approximate N^3LO parton distribution functions. We show numerical results at LHC energies of resummed q_T distributions for Z/γ^* , W^\pm production and decay, including the W^\pm and Z/γ^* ratio, estimating the corresponding uncertainties from missing higher orders corrections and from incomplete or missing perturbative information coefficients at N^4LL and N^4LO . Our resummed calculation has been encoded in the public numerical program **DYTurbo**.

© 2023 The Author(s). Published by Elsevier B.V. This is an open access article under the CC BY license (<http://creativecommons.org/licenses/by/4.0/>). Funded by SCOAP³.

The production of high invariant mass (M) lepton pairs in hadronic collision, through the Drell–Yan (DY) mechanism [1,2], is extremely important for physics studies at hadron colliders and attracted a great deal of attention from the experimental and theory communities. Since the early days of QCD remarkable efforts have been devoted to detailed calculations of the dominant QCD higher-order radiative corrections of fiducial cross sections and kinematical distributions.

A sufficiently inclusive cross section can be perturbatively computable as an expansion in the QCD coupling $\alpha_S = \alpha_S(\mu_R^2)$ where the renormalization scale μ_R is of the order of the invariant mass M . However the bulk of experimental data lies in the small transverse momentum (q_T) region $q_T \ll M$ where the fixed-order expansion is spoiled by the presence of enhanced logarithmic corrections, $\alpha_S^n \ln^m(M^2/q_T^2)$ of soft and collinear origin. In order to obtain reliable predictions, these logarithmic terms have to be systematically resummed to all orders in perturbation theory [3–5] (resummed calculation and studies applying different formalism and various levels of theoretical accuracy have been performed in Refs. [6–33]).

In this paper we consider the Drell–Yan lepton pair production in the small q_T region and we apply the QCD transverse-momentum resummation formalism developed in Refs. [6,8,17]. We resum all the logarithmically enhanced contributions up to the next-to-next-to-next-to-next-to-leading logarithmic (N^4LL) accuracy and we include the hard-virtual coefficient at the next-to-next-to-next-to-leading order (N^3LO) (i.e. $\mathcal{O}(\alpha_S^3)$) with an estimate of the N^4LO effects.

In the Z boson case, because of the axial coupling, Feynman diagrams with quark loops contribute to the cross-section at $\mathcal{O}(\alpha_S^2)$ and $\mathcal{O}(\alpha_S^3)$. These contributions, also known as singlet contributions, cancel out for each isospin multiplet when massless quarks are considered. The effect of a finite top-quark mass in the third generation has been considered at $\mathcal{O}(\alpha_S^2)$ in Refs. [34,35] and has been found extremely small compared to the NNLO corrections. However these effects are not completely negligible when compared to the N^3LO corrections [30]. We have considered the effect of a finite top-quark mass including in our calculation the singlet contributions up to $\mathcal{O}(\alpha_S^3)$ by using the calculation of the quark axial form factor in QCD up to three loops [36]. We consistently included also the quark-loop mediated three-loop singlet corrections which contribute, via vector coupling, both to Z and γ^* production at $\mathcal{O}(\alpha_S^3)$ [37,38].

* Corresponding author.

E-mail address: giancarlo.ferrera@mi.infn.it (G. Ferrera).

At large value of q_T ($q_T \sim M$) fixed-order perturbative expansion is fully justified. In this region, the QCD radiative corrections are known up to $\mathcal{O}(\alpha_S^3)$ numerically through the fully exclusive NNLO calculation of vector boson production in association with jets [31, 39–46]. In particular the calculation of $Z + \text{jet}$ production at NNLO has been encoded in the public code MCFM [31]. Resummed and fixed-order calculation have to be consistently (i.e. avoiding double counting) matched at intermediate values of q_T in order to obtain theoretical predictions with uniform accuracy over the entire range of q_T .

Our resummed calculation for Z/γ^* and W^\pm production and decay up to approximated $N^4\text{LL}+N^4\text{LO}$ accuracy, together with the asymptotic expansion up to $\mathcal{O}(\alpha_S^3)$, has been implemented in the public numerical program DYTurbo [47,48] which provides fast and numerically precise predictions including the full kinematical dependence of the decaying lepton pair with the corresponding spin correlations and the finite value of the Z boson width.

In this paper we are focusing on the impact of the $N^4\text{LL}$ resummed logarithmic terms. We thus consider only the small q_T region and we not include the matching with fixed-order predictions which can be implemented starting from the results of Refs. [31,39–46] and subtracting the *asymptotic* expansion of the resummed calculation at the same perturbative order as encoded in DYTurbo. Resummed results at $N^3\text{LL}+N^3\text{LO}$ matched with the NNLO calculation at large q_T have been presented in Refs. [49]. Here we improve the results of Ref. [49] by extending the resummation accuracy at approximated $N^4\text{LL}+N^4\text{LO}$ ¹ and by presenting results for W^\pm boson production and decay.

We consider the process

$$h_1 + h_2 \rightarrow V + X \rightarrow l_3 + l_4 + X, \quad (1)$$

where V denotes the vector boson produced by the colliding hadrons h_1 and h_2 with a centre-of-mass energy s , while l_3 and l_4 are the final state leptons produced by the V decay. The lepton kinematics is completely specified in terms of the transverse-momentum \mathbf{q}_T (with $q_T = \sqrt{\mathbf{q}_T^2}$), the rapidity y and the invariant mass M of the lepton pair, and by two additional variables Ω that specify the angular distribution of the leptons with respect to the vector boson momentum.

We consider the Drell-Yan cross section fully differential in the leptonic final state. According to the factorization theorem we can write

$$\frac{d\sigma_{h_1 h_2 \rightarrow l_3 l_4}}{d^2 \mathbf{q}_T dM^2 dy d\Omega} (\mathbf{q}_T, M^2, y, s, \Omega) = \sum_{a_1, a_2} \int_0^1 dx_1 \int_0^1 dx_2 f_{a_1/h_1}(x_1, \mu_F^2) f_{a_2/h_2}(x_2, \mu_F^2) \times \frac{d\hat{\sigma}_{a_1 a_2 \rightarrow l_3 l_4}}{d^2 \mathbf{q}_T dM^2 d\hat{y} d\Omega} (\mathbf{q}_T, M, \hat{y}, \hat{s}, \Omega; \alpha_S, \mu_R^2, \mu_F^2), \quad (2)$$

where $f_{a/h}(x, \mu_F^2)$ ($a = q_f, \bar{q}_f, g$) are the parton distribution functions of the hadron h , $\hat{s} = x_1 x_2 s$ is the partonic centre-of-mass energy squared, $\hat{y} = y - \ln \sqrt{x_1/x_2}$ is the vector boson rapidity with respect to the colliding partons while μ_R and μ_F are the renormalization and factorization scales. The last factor in the right-hand side of Eq. (2) is multi-differential partonic cross sections, computable in perturbative QCD as a series expansion in the strong coupling $\alpha_S = \alpha_S(\mu_R)$, which will be denoted in the following by the shorthand notation $[d\hat{\sigma}_{a_1 a_2 \rightarrow l_3 l_4}]$.

The partonic cross section can be decomposed as

$$[d\hat{\sigma}_{a_1 a_2 \rightarrow l_3 l_4}] = [d\hat{\sigma}_{a_1 a_2 \rightarrow l_3 l_4}^{(\text{res.})}] + [d\hat{\sigma}_{a_1 a_2 \rightarrow l_3 l_4}^{(\text{fin.})}] \quad (3)$$

where the first term on the right-hand side of Eq. (3) is the resummed component which dominates in the small q_T region while the second term is the finite component which is needed at large q_T .

A brief review of the resummation formalism of Refs. [6,8,17] is given in Appendix A together with a collection of the numerical coefficients needed at $N^4\text{LL}+N^4\text{LO}$ accuracy.

In the following we consider Z/γ^* , W^\pm production and leptonic decay at the Large Hadron Collider (LHC). We present resummed predictions up to $N^4\text{LL}$ accuracy including the hard-virtual coefficient up to $N^3\text{LO}$ together with an approximation of the $N^4\text{LO}$ ones. The hadronic cross section is obtained by convoluting the partonic cross section in Eq. (3) with the parton densities functions (PDFs) from MSHT20aN3LO set [50] at the approximate $N^3\text{LO}$ with $\alpha_S(m_Z^2) = 0.118$ where we have evaluated $\alpha_S(\mu_R^2)$ at $(n+1)$ -loop order at $N^n\text{LL}$ accuracy. We use the so-called G_μ scheme for EW couplings with input parameters $G_F = 1.1663787 \times 10^{-5}$ GeV $^{-2}$, $m_Z = 91.1876$ GeV, $\Gamma_Z = 2.4952$ GeV, $m_W = 80.379$ GeV, $\Gamma_W = 2.091$ GeV. In the case of W production, we use the following CKM matrix elements: $V_{ud} = 0.97427$, $V_{us} = 0.2253$, $V_{ub} = 0.00351$, $V_{cd} = 0.2252$, $V_{cs} = 0.97344$, $V_{cb} = 0.0412$. We work with $N_f = 5$ massless quarks and we use $m_{top} = 173$ GeV for the top-loop mediated singlet contributions. Our calculation implements the leptonic decays $Z/\gamma^* \rightarrow l^+ l^-$, $W^\pm \rightarrow l\nu$ and we include the effects of the Z/γ^* interference and of the finite widths of the W and Z boson with the corresponding spin correlations and the full dependence on the kinematical variables of final state leptons. This allows us to take into account the typical kinematical cuts on final state leptons that are considered in the experimental analysis. The resummed calculation at fixed lepton momenta requires a q_T -recoil procedure. We implement the general procedure described in Ref. [17] which is equivalent to compute the Born level distribution $d\sigma^{(0)}$ of Eq. (8) in the Collins-Soper rest frame [51].

As for the non-perturbative (NP) effects at very small transverse momenta we introduced, in the conjugated b -space, a NP form factor of the form [16]

$$S_{NP}(b) = \exp\{-g_1 b^2 - g_K(b) \ln(M^2/Q_0^2)\} \quad (4)$$

¹ We note that we are using the definition of labels introduced in Ref. [17]. In particular the fixed-order labels NLO, NNLO, $N^3\text{LO}$ and (approximated) $N^4\text{LO}$ refer to the perturbative accuracy in the small- q_T region and not to the perturbative accuracy in the large- q_T region.

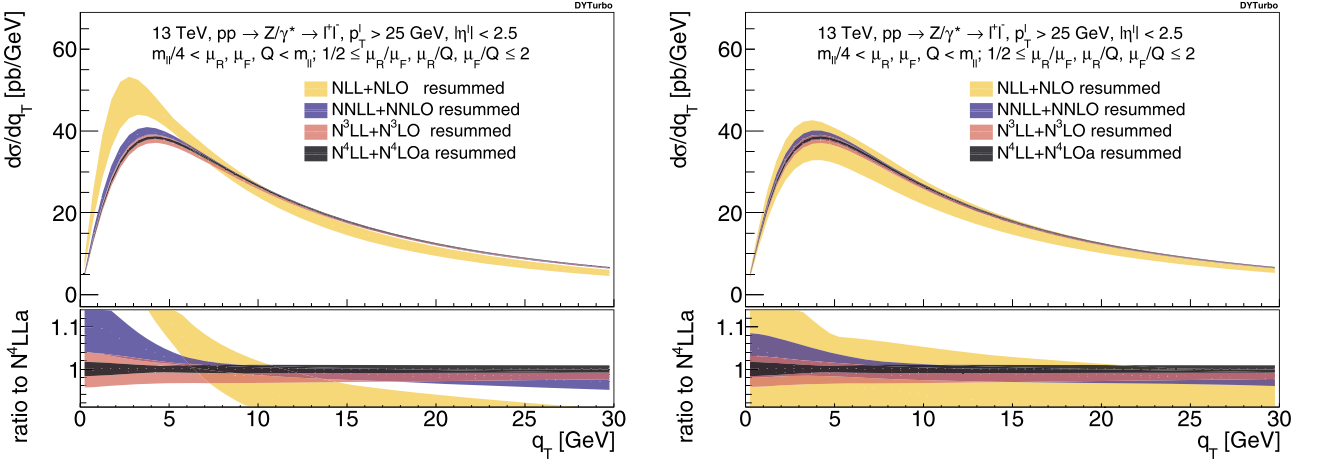


Fig. 1. The q_T spectrum of Z/γ^* bosons with lepton selection cuts at the LHC ($\sqrt{s} = 13$ TeV) at various perturbative orders. Resummed component (see Eq. (3)) of the hadronic cross-section with scale variation bands as defined in the text. The order of the parton density evolution is set consistently with the order of the resummation (left) or with the order of the PDFs (right).

where

$$g_K(b) = g_0 \left(1 - \exp \left[-\frac{C_F \alpha_S((b_0/b_*)^2) b^2}{\pi g_0 b_{\text{lim}}^2} \right] \right), \quad (5)$$

with $g_1 = 0.5$ GeV 2 , $Q_0 = 1$ GeV, $g_0 = 0.3$, $b_{\text{lim}} = 1.5$ GeV $^{-1}$ and

$$b_*^2 = b^2 b_{\text{lim}}^2 / (b^2 + b_{\text{lim}}^2). \quad (6)$$

The g_1 parameter controls the quadratic NP power corrections which are dominant in the region of moderate q_T of 4–10 GeV while g_0 controls the asymptotic behaviour of the NP form factor at very small q_T . The parameter b_{lim} set the scale at which the running of α_S in Eq. (5) is frozen while Q_0 represent the initial scale at which the NP form factor is parameterised. The variable b_* is also used to regularize the perturbative form factor at very large value of b ($b \gtrsim 1/\Lambda_{QCD}$, where Λ_{QCD} is the scale of the Landau pole of the running coupling $\alpha_S(q^2)$) which correspond to very small values of q_T ($q_T \lesssim \Lambda_{QCD}$) through the so-called ‘ b_* prescription’ [5,52] which consist in the freezing of the integration over b below the upper limit b_{lim} through the replacement $b \rightarrow b_*$. An alternative regularization procedure of the Landau singularity, which have also been implemented in the DYTurbo numerical program, is the so-called Minimal Prescription [53–55] which avoid the Landau singularity by deforming the integration contour in the complex b space. The Minimal Prescription does not require any infrared cut-off, it leaves unchanged the perturbative result to any fixed order in α_S and it can be implemented within a purely perturbative framework without introducing an explicit model of NP effects.

We have thus considered the production of l^+l^- pairs from Z/γ^* decay at the LHC ($\sqrt{s} = 13$ TeV) with the following fiducial cuts: the leptons are required to have transverse momentum $p_T > 25$ GeV, pseudo-rapidity $|\eta| < 2.5$ while the lepton pair system is required to have an invariant mass of $80 < M_{l^+l^-} < 100$ GeV with transverse momentum $q_T < 30$ GeV.

In order to estimate the size of yet uncalculated higher-order terms and the ensuing perturbative uncertainties we consider the dependence of the results from the auxiliary scales μ_F , μ_R and Q . We thus perform an independent variation of μ_F , μ_R and Q in the range $M/2 \leq \{\mu_F, \mu_R, Q\} \leq 2M$ with the constraints $0.5 \leq \{\mu_F/\mu_R, Q/\mu_R, Q/\mu_F\} \leq 2$.

In Fig. 1 we consider Z/γ^* production and decay and we show the resummed component (see Eq. (3)) of the transverse-momentum distribution in the small- q_T region. The label N^nLL+N^nLO ($n = 1, 2, 3$) indicates that we perform the resummation of logarithmic enhanced contribution at N^nLL accuracy including the hard-virtual coefficient at N^nLO while the label N^4LL+N^4LOa indicates that we perform the resummation at N^4LL accuracy with the hard-virtual coefficient at N^4LO and an estimate of yet not known N^4LO corrections.²

In the left panel of Fig. 1 we show the resummed predictions following the original formalism of Refs. [6,8,17]. The lower panel shows the ratio of the distribution with respect to the N^4LLa prediction at the central value of the scales $\mu_F = \mu_R = Q = M$. We observe that the NLL+NLO and NNLL+NNLO scale dependence bands do not overlap thus showing that the NLL+NLO scale variation underestimates the true perturbative uncertainty. This feature was already observed and discussed in Refs. [17,49]. In the present case the lack of overlap can be ascribed to the fact that we are using the same N^3LO parton densities set at NLL, NNLL, N^3LL and N^4LL accuracy. This choice introduces a formal mismatch between the N^3LO Altarelli-Parisi evolution as encoded in the N^3LO parton densities functions and the corresponding N^kLO evolution included in the $N^{k+1}LL$ partonic resummed formula.

In order to show that this is indeed the case, in the right panel of Fig. 1 we show the resummed predictions in which we set the order of Altarelli-Parisi evolution in the resummed prediction to be equal to the order of the parton densities (i.e. both at approximated N^3LO). In practice, with this choice, we are modifying the NLL, NNLL and N^3LL predictions by including formally subleading logarithmic corrections.³ We observe that with this choice the scale dependence bands show a nice overlap at subsequent orders thus indicating that

² Incidentally we observe that our prediction at N^4LL+N^4LOa includes the full perturbative information contained in the so-called N^4LL accuracy and also a reliable approximation of the N^4LL' accuracy as sometimes defined in the literature.

³ We note that this inclusion of formally subleading terms is similar to what happen in the Collins, Soper and Sterman resummation formalism [5] where the parton densities are evaluated at the scale b_0/b [4].

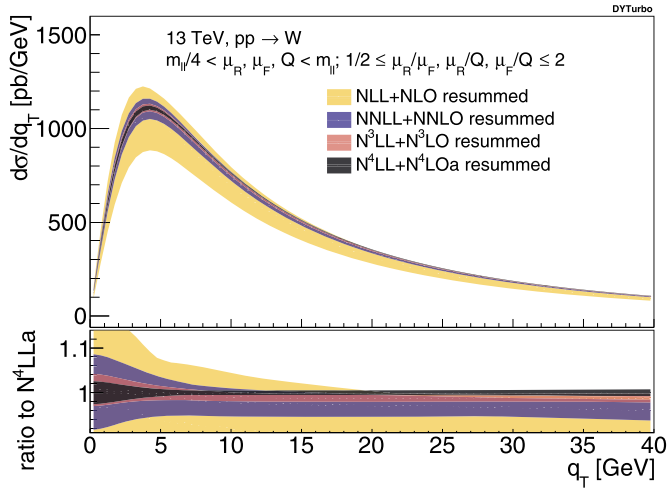


Fig. 2. The q_T spectrum of W^+ and W^- bosons with inclusive leptonic decay at the LHC ($\sqrt{s} = 13$ TeV) at various perturbative orders. Resummed component (see Eq. (3)) of the hadronic cross-section with scale variation bands as defined in the text.

the lack of overlap of the previous case is indeed related to the mismatch in the order of the evolution of parton densities. However we also note that by keeping fixed the evolution of the parton densities at subsequent orders inevitably underestimates the impact of higher order corrections included in the PDFs.

Finally, we observe that the choice of the order in the evolution of parton densities only affects the NLL+NLO and, with a minor extent, NNLO+NNLO theoretical predictions and corresponding uncertainties. Its impact is negligible at N^3LL+N^3LO (the N^4LL+N^4LOa prediction is independent by the choice). Since we are mainly interested on the impact of N^4LL+N^4LOa corrections with respect to the N^3LL+N^3LO results in the following we show numerical results only for the case in which the order of evolution of parton densities is set consistently with the order of the PDF set.

In both the left and right panel of Fig. 1 the scale dependence is consistently reduced increasing the perturbative order, in particular it is roughly reduced by a factor of 2 going from N^3LL to N^4LLa . The scale variation at N^4LLa accuracy is around $\pm 1.5\%$ at $q_T \sim 1$ GeV, then it reduces at $\pm 1\%$ level at the peak ($q_T \sim 4$ GeV) and remains roughly constant up to $q_T \sim 30$ GeV.

In the results of Fig. 1 we considered the effect of a finite top-quark mass including the singlet contributions mediated by heavy-quark loops at NNLO and N^3LO . As already found in the literature [34,35] the impact of these contributions is extremely small, the effect is of -0.04% at NNLO and less than $+0.001\%$ at N^3LO . Given the negligible effect of the singlet contributions at N^3LO , we have not estimated the impact of singlet contributions at N^4LO .

In Fig. 2 we consider W boson production and decay into a $l\nu_l$ pair showing the resummed component of the transverse-momentum distribution in the small- q_T region at different perturbative orders. In this case we do not consider kinematical selection cuts apart a lower limit of 50 GeV on the invariant mass of the vector boson (lepton pair) which is necessary in order to fix a hard scale for the process. Also in this case we observe that the scale dependence is consistently reduced increasing the perturbative order. The scale variation at N^4LLa accuracy is around $\pm 2\%$ at $q_T \sim 1$ GeV, then it reduces at $\pm 1\%$ level at the peak ($q_T \sim 4$ GeV), decreases to $\pm 0.5\%$ for $q_T \sim 7$ GeV and remains below $\pm 1\%$ level up to $q_T \sim 30$ GeV.

The knowledge of the shape of the W boson q_T distribution and its uncertainty is particularly important since it affects the measurement of the W mass. However the W boson q_T spectrum is not directly experimental accessible with good resolution due to the neutrino in final state of the leptonic W decay. Conversely, the q_T spectrum of the Z boson has been measured with great precision. Therefore a precise theoretical prediction of the ratio of W and Z q_T distributions, together with the measurement of the Z boson q_T spectrum, gives stringent information on the W spectrum.

In Fig. 3 we consider the ratio of q_T distributions for Z/γ^* and W^\pm production and decay. We consider the quantity

$$R(q_T) = \frac{\sigma_Z}{\sigma_W} \frac{d\sigma_W}{dq_T} / \frac{d\sigma_Z}{dq_T}, \quad (7)$$

where $\frac{1}{\sigma_V} \frac{d\sigma_V}{dq_T}$ with $V = W, Z$ is the normalized q_T distribution for W and Z/γ^* production and decay inclusive over the leptonic final state kinematics, apart for a selection cut on the invariant mass of the lepton pair: $80 < M_{l^+l^-} < 100$ GeV and $M_{l\nu} > 50$ GeV.

In Fig. 3 we show the resummed component of the transverse-momentum distribution of Eq. (7) for the ratio W^+/Z (left panel) and W^-/Z (right panel) in the small- q_T region. From the results of Fig. 3 (left and right panels) we observe that the scale dependence is greatly reduced (roughly by one order of magnitude) with respect to the distributions shown in Figs. 1, 2. The scale variation at N^4LL+N^4LOa accuracy is around $\pm 0.3\% - 0.4\%$ at $q_T \sim 1$ GeV, then it reduces at $\pm 0.1\%$ level at the peak ($q_T \sim 4$ GeV), it further decrease below 0.05% level for $q_T \sim 7$ GeV and then it slightly increases up to $\pm 0.2\%$ for $q_T \sim 30$ GeV. This reduction of scale uncertainty is not unexpected because in the ratio correlated uncertainties on W and Z distributions cancel. In particular higher order QCD predictions for the resummed component of the cross section has a high degree of universality and the process dependence is mainly due to the different flavour content of the partonic subprocesses for W and Z production.

One may wonder if correlated scale variation for the ratio of W and Z distribution can underestimate the true perturbative uncertainty. A way to assess the consistency of the use of perturbative scale variation in estimating the perturbative uncertainty from missing higher orders is to check it by explicit calculation i.e. verifying if the next-order calculation lies within the scale variation bands at a given order. If this is the case it means that scale variation, at that order, correctly estimates the size of next-order corrections. Of course this procedure

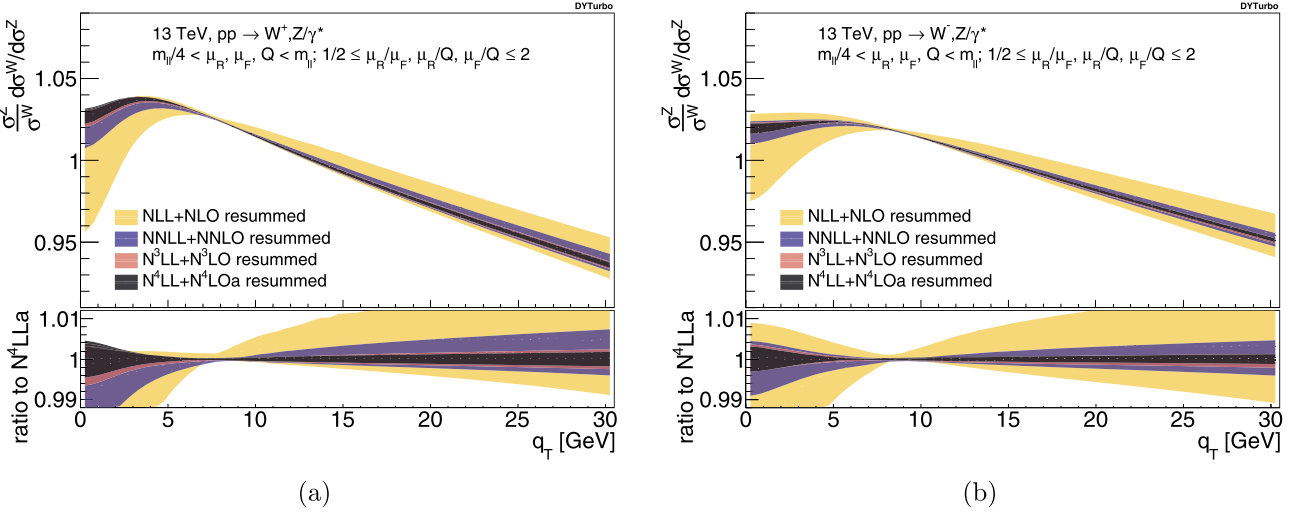


Fig. 3. The normalized ratio of q_T spectra of W and Z/γ^* bosons at the LHC ($\sqrt{s} = 13$ TeV) at various perturbative orders for W^+/Z (left) and W^-/Z (right). Resummed component (see Eq. (3)) of the hadronic cross-section with scale variation bands as defined in the text.

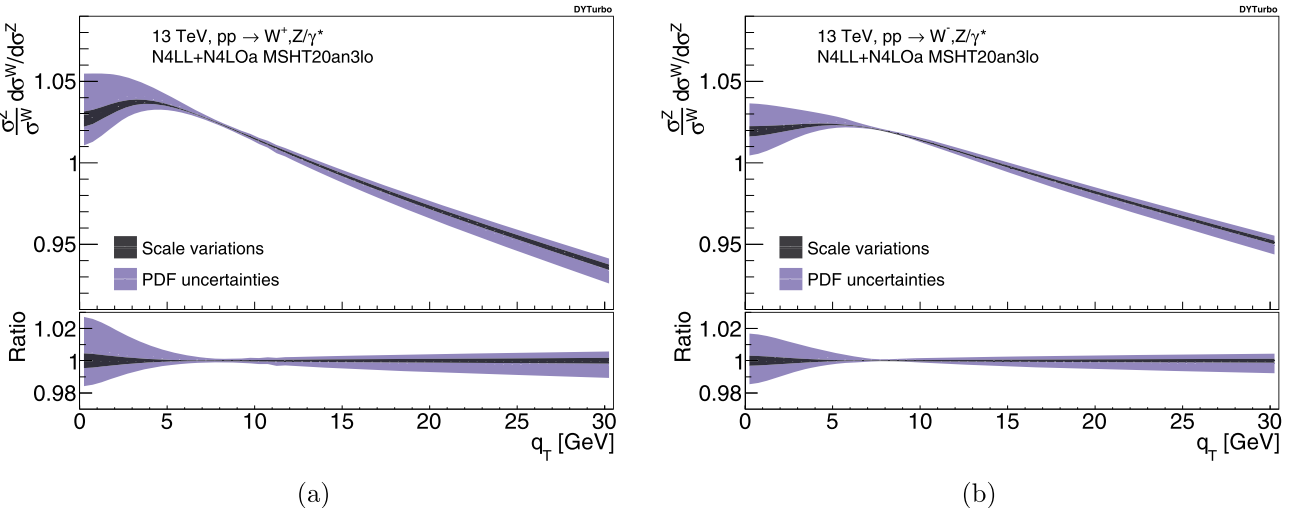


Fig. 4. The normalized ratio of q_T spectra of W and Z/γ^* bosons at the LHC ($\sqrt{s} = 13$ TeV) at N^4LL+N^4LOa accuracy for W^+/Z (left) and W^-/Z (right). Resummed component (see Eq. (3)) of the hadronic cross-section with scale variation band as defined in the text and PDF uncertainty from MSHT20aN3LO set.

can only be applied *a posteriori* leaving the scale uncertainty band at the last known order as a *reasonable estimate* of the true perturbative uncertainty. In the present case the overlap of the scale uncertainty band indicates that correlated scale variation at NLL+NLO, NNLL+NNLO and N^3LL+N^3LO correctly estimate the size of higher-order corrections thus leaving us confident on the reliability of the N^4LL+N^4LO scale variation band.⁴ An alternative, and more robust, perturbative uncertainty can be obtained considering the size of the difference between the prediction at a given order with respect to the prediction at the previous order. In this way we obtain an uncertainty which is even smaller than the one obtained through the perturbative scale variation method.

However we stress that the predictions presented in Fig. 3 are far from being complete since at such level of theoretical precision several effects cannot be neglected. In particular also very small effects which however are different in the W and Z case can give not negligible effects on the W/Z ratio. For instance the impact of the *process dependent* finite component of the cross section, the (flavour dependent) non-perturbative *intrinsic k_T* effects [56], the QED and electroweak effects [57–61], the heavy-quark mass effects [62–65]. Another important source of uncertainty is the one arising from the determination of PDFs. An estimate of such uncertainty is typically provided in global PDF fits. In Fig. 4 we show the impact of the PDFs uncertainty from MSHT20aN3LO set [50] on the prediction for the W^+/Z (left panel) and W^-/Z (right panel) ratio. We observe that the PDF uncertainty dominates over the scale variation band being larger by roughly a factor of 4.

In conclusion, in this paper we have presented the implementation of the q_T resummation formalism of Refs. [6,8,17] for Drell-Yan processes up to N^4LL+N^4LO approximated accuracy in the DYTurbo numerical program [47,48]. We have illustrated explicit numerical results for the resummed component of the transverse-momentum distribution for the case of Z/γ^* , W^\pm production and leptonic decay

⁴ We have also checked that adopting a more conservative *uncorrelated* scale variation prescription would produce a scale uncertainty band which largely overestimate the size of higher-order corrections (see also the results of Ref. [22]).

at LHC energies. We also considered theoretical predictions for the ratio of W^\pm and Z/γ^* q_T distributions. Perturbative uncertainties have been estimated through a study of the scale variation band.

In Appendix A we provide an estimate of the uncertainties arising from the numerical approximations of the N^4LL coefficients, and from the incomplete knowledge of the N^4LO perturbative coefficients. The size of the unknown N^4LO coefficients and its associated uncertainty is estimated through a Levin transform of the corresponding perturbative series [66,67]. The dominant uncertainties are the numerical approximations of the 4-loop singlet splitting functions [68,69] and the incomplete knowledge of the hard-collinear coefficients [70] at 4 loops which amount, in both cases, to $1\text{--}3 \cdot 10^{-3}$ relative uncertainty. These uncertainties turn out to be 5 to 10 times smaller compared to the perturbative uncertainties estimated through scale variations.

The **DYTurbo** numerical code allows the user to apply arbitrary kinematical cuts on the vector boson and the final-state leptons, and to compute the corresponding relevant distributions in the form of bin histograms. These features make **DYTurbo** a useful tool for Drell-Yan studies at hadron colliders such as the Tevatron and the LHC.

Declaration of competing interest

The authors declare that they have no known competing financial interests or personal relationships that could have appeared to influence the work reported in this paper.

Data availability

No data was used for the research described in the article.

Acknowledgements

LC is supported by the Generalitat Valenciana (Spain) through the plan GenT program (CIDEgent/2020/011) and his work is supported by the Spanish Government (Agencia Estatal de Investigación) and ERDF funds from European Commission (Grant no. PID2020-114473GB-I00 funded by MCIN/AEI/10.13039/501100011033).

Appendix A. Transverse-momentum resummation up to N^4LL+N^4LO accuracy

We briefly review the impact-parameter space b [4] resummation formalism of Refs. [6,8,17]. The resummed component in the r.h.s. of Eq. (3) can then be written as

$$\left[d\hat{\sigma}_{a_1 a_2 \rightarrow l_3 l_4}^{(\text{res.})} \right] = \sum_{b_1, b_2 = q, \bar{q}} \frac{d\hat{\sigma}_{b_1 b_2 \rightarrow l_3 l_4}^{(0)}}{d\Omega} \frac{1}{\hat{s}} \int_0^\infty \frac{db}{2\pi} b J_0(bq_T) \mathcal{W}_{a_1 a_2, b_1 b_2 \rightarrow V}(b, M, \hat{y}, \hat{s}; \alpha_S, \mu_R^2, \mu_F^2), \quad (8)$$

where $J_0(x)$ is the 0th-order Bessel function and the factor $d\hat{\sigma}_{b_1 b_2 \rightarrow l_3 l_4}^{(0)}$ is the Born level differential cross section for the partonic subprocess $q\bar{q} \rightarrow V \rightarrow l_3 l_4$.

The function $\mathcal{W}_V(b, M, \hat{y}, \hat{s})$ can be expressed in an exponential form by considering the ‘double’ (N_1, N_2) Mellin moments with respect to the variables $z_1 = e^{+\hat{y}} M / \sqrt{\hat{s}}$ and $z_2 = e^{-\hat{y}} M / \sqrt{\hat{s}}$ at fixed M^5 [6,71]

$$\mathcal{W}_V(b, M; \alpha_S, \mu_R^2, \mu_F^2) = \mathcal{H}_V(\alpha_S; M/\mu_R, M/\mu_F, M/Q) \times \exp\{\mathcal{G}(\alpha_S, L; M/\mu_R, M/Q)\}, \quad (9)$$

where we have introduced the logarithmic expansion parameter

$$L \equiv \ln(Q^2 b^2 / b_0^2) \quad (10)$$

with $b_0 = 2e^{-\gamma_E}$ ($\gamma_E = 0.5772\dots$ is the Euler number). The scale $Q \sim M$ is the resummation scale [72], which parameterizes the arbitrariness in the resummation procedure.

The process dependent function $\mathcal{H}_V(\alpha_S)$ [73,74] includes the hard-collinear contributions and it can be written in term of a process dependent hard factor $H_V(\alpha_S)$ and two process independent functions $C(\alpha_S)$ associated to collinear emissions from the initial state colliding partons⁶

$$\mathcal{H}_V(\alpha_S) = H_V(\alpha_S) C(\alpha_S) C(\alpha_S). \quad (11)$$

The functions in Eq. (11) have a standard perturbative expansion

$$\mathcal{H}_V(\alpha_S) = 1 + \sum_{n=1}^{\infty} \left(\frac{\alpha_S}{\pi} \right)^n \mathcal{H}_V^{(n)}, \quad (12)$$

$$H_V(\alpha_S) = 1 + \sum_{n=1}^{\infty} \left(\frac{\alpha_S}{\pi} \right)^n H_V^{(n)}, \quad (13)$$

⁵ For the sake of simplicity in our symbolic notation the explicit dependence on parton indices (which are relevant for the exponentiation in the multiflavour space) and the double Mellin indices are understood. The interested reader can find the details in Ref. [6] (in particular Appendix A) and Ref. [71].

⁶ A simple specification of a resummation scheme customarily used in the literature on q_T resummation for vector boson is: $H_V(\alpha_S) \equiv 1$ (i.e. $H_V^{(n)} = 0$ for $n > 0$).

$$C(\alpha_S) = 1 + \sum_{n=1}^{\infty} \left(\frac{\alpha_S}{\pi} \right)^n C^{(n)}, \quad (14)$$

therefore up to the fourth order we have the following relations

$$\mathcal{H}_V^{(1)} = H_V^{(1)} + C^{(1)} + C^{(1)}, \quad (15)$$

$$\mathcal{H}_V^{(2)} = H_V^{(2)} + C^{(2)} + C^{(2)} + H_V^{(1)}(C^{(1)} + C^{(1)}) + C^{(1)}C^{(1)}, \quad (16)$$

$$\begin{aligned} \mathcal{H}_V^{(3)} &= H_V^{(3)} + C^{(3)} + C^{(3)} + H_V^{(2)}(C^{(1)} + C^{(1)}) + H_V^{(1)}(C^{(2)} + C^{(2)} + C^{(1)}C^{(1)}) \\ &\quad + C^{(2)}C^{(1)} + C^{(2)}C^{(1)}, \end{aligned} \quad (17)$$

$$\begin{aligned} \mathcal{H}_V^{(4)} &= H_V^{(4)} + C^{(4)} + C^{(4)} + H_V^{(3)}(C^{(1)} + C^{(1)}) + H_V^{(2)}(C^{(2)} + C^{(2)} + C^{(1)}C^{(1)}) \\ &\quad + H_V^{(1)}(C^{(3)} + C^{(3)} + C^{(2)}C^{(1)} + C^{(2)}C^{(1)}) + C^{(3)}C^{(1)} + C^{(3)}C^{(1)} + C^{(2)}C^{(2)}. \end{aligned} \quad (18)$$

The universal (process independent) form factor $\exp\{\mathcal{G}\}$ in the right-hand side of Eq. (9) contains all the terms that order-by-order in α_S are logarithmically divergent as $b \rightarrow \infty$ (i.e. $q_T \rightarrow 0$). The resummed logarithmic expansion of \mathcal{G} reads [6]

$$\begin{aligned} \mathcal{G}(\alpha_S, L) &= - \int_{b_0^2/b^2}^{Q^2} \frac{dq^2}{q^2} \left[A(\alpha_S(q^2)) \ln \frac{M^2}{q^2} + \tilde{B}(\alpha_S(q^2)) \right] \\ &= L g^{(1)}(\alpha_S L) + g^{(2)}(\alpha_S L) + \sum_{n=1}^{\infty} \left(\frac{\alpha_S}{\pi} \right)^n g^{(n+2)}(\alpha_S L), \end{aligned} \quad (19)$$

where the functions $g^{(n)}$ control and resum the $\alpha_S^k L^k$ (with $k \geq 1$) logarithmic terms in the exponent of Eq. (9) due to soft and collinear radiation. The perturbative functions $A(\alpha_S)$ and $\tilde{B}(\alpha_S)$ can be expanded as

$$A(\alpha_S) = \sum_{n=1}^{\infty} \left(\frac{\alpha_S}{\pi} \right)^n A^{(n)}, \quad (20)$$

$$\tilde{B}(\alpha_S) = \sum_{n=1}^{\infty} \left(\frac{\alpha_S}{\pi} \right)^n \tilde{B}^{(n)}. \quad (21)$$

The function $\tilde{B}(\alpha_S)$ can be written as follows

$$\tilde{B}(\alpha_S) = B(\alpha_S) + 2\beta(\alpha_S) \frac{d \ln C(\alpha_S)}{d \ln \alpha_S} + 2\gamma(\alpha_S), \quad (22)$$

in terms of the resummation coefficient $B(\alpha_S)$, the collinear functions $C(\alpha_S)$ (see Eq. (14)), the functions $\gamma(\alpha_S)$ (the Mellin moments of the Altarelli–Parisi splitting functions⁷) and the QCD β function

$$\frac{d \ln \alpha_S(\mu^2)}{d \ln \mu^2} = \beta(\alpha_S) = - \sum_{n=0}^{+\infty} \beta_n \left(\frac{\alpha_S}{\pi} \right)^{n+1}. \quad (23)$$

By explicit integration of Eq. (19) we obtain the following $g^{(i)}$ for $1 \leq i \leq 5$

$$g^{(1)}(\alpha_S L) = \frac{A^{(1)}}{\beta_0} \frac{\lambda + \ln(1 - \lambda)}{\lambda}, \quad (24)$$

$$\begin{aligned} g^{(2)}(\alpha_S L) &= \frac{\overline{B}^{(1)}}{\beta_0} \ln(1 - \lambda) - \frac{A^{(2)}}{\beta_0^2} \left(\frac{\lambda}{1 - \lambda} + \ln(1 - \lambda) \right) \\ &\quad + \frac{A^{(1)}}{\beta_0} \left(\frac{\lambda}{1 - \lambda} + \ln(1 - \lambda) \right) \ln \frac{Q^2}{\mu_R^2} \\ &\quad + \frac{A^{(1)}\beta_1}{\beta_0^3} \left(\frac{1}{2} \ln^2(1 - \lambda) + \frac{\ln(1 - \lambda)}{1 - \lambda} + \frac{\lambda}{1 - \lambda} \right), \end{aligned} \quad (25)$$

⁷ In order to match the effect of the charm and bottom-mass threshold included in the evolution of PDFs in Eq. (2), the resummation (evolution) effects due to the $\gamma(\alpha_S)$ term in Eq. (19) are asymptotically switched off when approaching their corresponding quark-mass thresholds through a b_* prescription (see Eq. (6)) with values of $b_{\lim} = 1/m_q$ [75].

$$\begin{aligned}
g^{(3)}(\alpha_S L) = & -\frac{A^{(3)}}{2\beta_0^2} \frac{\lambda^2}{(1-\lambda)^2} - \frac{\bar{B}^{(2)}}{\beta_0} \frac{\lambda}{1-\lambda} + \frac{A^{(2)}\beta_1}{\beta_0^3} \left(\frac{\lambda(3\lambda-2)}{2(1-\lambda)^2} - \frac{(1-2\lambda)\ln(1-\lambda)}{(1-\lambda)^2} \right) \\
& + \frac{\bar{B}^{(1)}\beta_1}{\beta_0^2} \left(\frac{\lambda}{1-\lambda} + \frac{\ln(1-\lambda)}{1-\lambda} \right) - \frac{A^{(1)}}{2} \frac{\lambda^2}{(1-\lambda)^2} \ln^2 \frac{Q^2}{\mu_R^2} \\
& + \ln \frac{Q^2}{\mu_R^2} \left(\bar{B}^{(1)} \frac{\lambda}{1-\lambda} + \frac{A^{(2)}}{\beta_0} \frac{\lambda^2}{(1-\lambda)^2} + A^{(1)} \frac{\beta_1}{\beta_0^2} \left(\frac{\lambda}{1-\lambda} + \frac{1-2\lambda}{(1-\lambda)^2} \ln(1-\lambda) \right) \right) \\
& + A^{(1)} \left(\frac{\beta_1^2}{2\beta_0^4} \frac{1-2\lambda}{(1-\lambda)^2} \ln^2(1-\lambda) + \ln(1-\lambda) \left[\frac{\beta_0\beta_2-\beta_1^2}{\beta_0^4} + \frac{\beta_1^2}{\beta_0^4(1-\lambda)} \right] \right. \\
& \left. + \frac{\lambda}{2\beta_0^4(1-\lambda)^2} (\beta_0\beta_2(2-3\lambda) + \beta_1^2\lambda) \right), \tag{26}
\end{aligned}$$

$$\begin{aligned}
g^{(4)}(\alpha_S L) = & -\frac{A^{(4)}}{6\beta_0^2} \frac{(3-\lambda)\lambda^2}{(1-\lambda)^3} - \frac{\bar{B}^{(3)}}{2\beta_0} \frac{(2-\lambda)\lambda}{(1-\lambda)^2} - \frac{A^{(3)}}{2\beta_0} \left(\frac{\beta_1}{\beta_0^2} \left[\frac{(6-15\lambda+5\lambda^2)\lambda}{6(1-\lambda)^3} \right. \right. \\
& \left. \left. + \frac{(1-3\lambda)}{(1-\lambda)^3} \ln(1-\lambda) \right] - \frac{(3-\lambda)\lambda^2}{(1-\lambda)^3} \ln \frac{Q^2}{\mu_R^2} \right) + \bar{B}^{(2)} \left(\frac{\beta_1}{\beta_0^2} \left[\frac{(2-\lambda)\lambda}{2(1-\lambda)^2} + \frac{\ln(1-\lambda)}{(1-\lambda)^2} \right] \right. \\
& \left. + \frac{(2-\lambda)\lambda}{(1-\lambda)^2} \ln \frac{Q^2}{\mu_R^2} \right) + A^{(2)} \left(-\frac{2\beta_2}{3\beta_0^3} \frac{\lambda^3}{(1-\lambda)^3} + \frac{\beta_1^2}{2\beta_0^4} \left(\frac{\lambda(6-9\lambda+11\lambda^2)}{6(1-\lambda)^3} + \frac{\ln(1-\lambda)}{(1-\lambda)^2} \right. \right. \\
& \left. \left. + \frac{1-3\lambda}{(1-\lambda)^3} \ln^2(1-\lambda) \right) + \left[\frac{\beta_1}{2\beta_0^2} \frac{(2-\lambda)\lambda}{(1-\lambda)^2} + \frac{\beta_1}{\beta_0^2} \frac{1-3\lambda}{(1-\lambda)^3} \ln(1-\lambda) \right] \ln \frac{Q^2}{\mu_R^2} \right. \\
& \left. - \frac{(3-\lambda)\lambda^2}{2(1-\lambda)^3} \ln^2 \frac{Q^2}{\mu_R^2} \right) + \bar{B}^{(1)} \left(\frac{\beta_1^2}{2\beta_0^3} \left[\frac{\lambda^2}{(1-\lambda)^2} - \frac{\ln^2(1-\lambda)}{(1-\lambda)^2} \right] - \frac{\beta_2}{2\beta_0^2} \frac{\lambda^2}{(1-\lambda)^2} \right. \\
& \left. - \frac{\beta_1 \ln(1-\lambda)}{\beta_0 (1-\lambda)^2} \ln \frac{Q^2}{\mu_R^2} - \frac{\beta_0}{2} \frac{(2-\lambda)\lambda}{(1-\lambda)^2} \ln^2 \frac{Q^2}{\mu_R^2} \right) + A^{(1)} \left(-\frac{\beta_1^3}{\beta_0^5} \left(\frac{\lambda^3}{6(1-\lambda)^3} \right. \right. \\
& \left. \left. + \frac{(1+\lambda)\lambda^2}{2(1-\lambda)^3} \ln(1-\lambda) + \frac{\lambda}{2(1-\lambda)^3} \ln^2(1-\lambda) + \frac{(1-3\lambda)}{6(1-\lambda)^3} \ln^3(1-\lambda) \right) \right. \\
& \left. - \frac{\beta_1\beta_2}{2\beta_0^4} \left(\frac{\lambda(6-15\lambda+5\lambda^2)}{6(1-\lambda)^3} + \frac{(1-3\lambda+2\lambda^2-2\lambda^3)}{(1-\lambda)^3} \ln(1-\lambda) \right) \right. \\
& \left. + \frac{\beta_3}{2\beta_0^3} \left(\frac{\lambda(6-15\lambda+7\lambda^2)}{6(1-\lambda)^3} + \ln(1-\lambda) \right) + \left[-\frac{\beta_1^2}{\beta_0^3} \left(\frac{\lambda^2(1+\lambda)}{2(1-\lambda)^3} + \frac{\lambda}{(1-\lambda)^3} \ln(1-\lambda) \right) \right. \right. \\
& \left. \left. + \frac{1-3\lambda}{2(1-\lambda)^3} \ln^2(1-\lambda) \right] + \frac{\beta_2}{2\beta_0^2} \frac{\lambda^2(1+\lambda)}{(1-\lambda)^3} \right] \ln \frac{Q^2}{\mu_R^2} - \frac{\beta_1}{2\beta_0} \left[\frac{\lambda}{(1-\lambda)^3} \right. \\
& \left. + \frac{1-3\lambda}{(1-\lambda)^3} \ln(1-\lambda) \right] \ln^2 \frac{Q^2}{\mu_R^2} + \frac{\beta_0}{6} \frac{(3-\lambda)\lambda^2}{(1-\lambda)^3} \ln^3 \frac{Q^2}{\mu_R^2}, \tag{27}
\end{aligned}$$

$$\begin{aligned}
g^{(5)}(\alpha_S L) = & -\frac{A^{(5)}}{12\beta_0^2} \frac{\lambda^2(6-4\lambda+\lambda^2)}{(1-\lambda)^4} - \frac{\bar{B}^{(4)}}{3\beta_0} \frac{\lambda(3-3\lambda+\lambda^2)}{(1-\lambda)^3} \\
& + \frac{A^{(4)}}{3\beta_0} \left(\frac{\beta_1}{\beta_0^2} \left[\frac{\lambda(-12+42\lambda-28\lambda^2+7\lambda^3)}{12(1-\lambda)^4} - \frac{1-4\lambda}{(1-\lambda)^4} \ln(1-\lambda) \right] \right. \\
& \left. + \frac{\lambda^2(6-4\lambda+\lambda^2)}{(1-\lambda)^4} \ln \frac{Q^2}{\mu_R^2} \right) + \bar{B}^{(3)} \left(\frac{\beta_1}{\beta_0^2} \left[\frac{\lambda(3-3\lambda+\lambda^2)}{3(1-\lambda)^3} + \frac{\ln(1-\lambda)}{(1-\lambda)^3} \right] \right. \\
& \left. + \frac{\lambda(3-3\lambda+\lambda^2)}{(1-\lambda)^3} \ln \frac{Q^2}{\mu_R^2} \right) + A^{(3)} \left(-\frac{\beta_2}{4\beta_0^3} \frac{\lambda^3(4-\lambda)}{(1-\lambda)^4} \right. \\
& \left. + \frac{\beta_1^2}{\beta_0^4} \left[\frac{\lambda(12-24\lambda+52\lambda^2-13\lambda^3)}{36(1-\lambda)^4} + \frac{\ln(1-\lambda)}{3(1-\lambda)^3} + \frac{1-4\lambda}{2(1-\lambda)^4} \ln^2(1-\lambda) \right] \right. \\
& \left. + \frac{\beta_1}{\beta_0^2} \left[\frac{\lambda(3-3\lambda+\lambda^2)}{3(1-\lambda)^3} + \frac{1-4\lambda}{(1-\lambda)^4} \ln(1-\lambda) \right] \ln \frac{Q^2}{\mu_R^2} \right)
\end{aligned}$$

$$\begin{aligned}
& - \frac{\lambda^2(6-4\lambda+\lambda^2)}{2(1-\lambda)^4} \ln^2 \frac{Q^2}{\mu_R^2} \Bigg) + \overline{B}^{(2)} \left(- \frac{\beta_2}{3\beta_0^2} \frac{(3-\lambda)\lambda^2}{(1-\lambda)^3} + \frac{\beta_1^2}{\beta_0^3} \left(\frac{(3-\lambda)\lambda^2}{3(1-\lambda)^3} \right. \right. \\
& - \frac{\ln^2(1-\lambda)}{(1-\lambda)^3} \Big) - \frac{2\beta_1}{\beta_0} \frac{\ln(1-\lambda)}{(1-\lambda)^3} \ln \frac{Q^2}{\mu_R^2} - \beta_0 \frac{\lambda(3-3\lambda+\lambda^2)}{(1-\lambda)^3} \ln^2 \frac{Q^2}{\mu_R^2} \Big) \\
& + A^{(2)} \left(- \frac{\beta_3}{12\beta_0^3} \frac{\lambda^3(8-5\lambda)}{(1-\lambda)^4} + \frac{\beta_1\beta_2}{3\beta_0^4} \left(\frac{\lambda(6-21\lambda+44\lambda^2-20\lambda^3)}{6(1-\lambda)^4} \right. \right. \\
& + \frac{1-4\lambda+9\lambda^2}{(1-\lambda)^4} \ln(1-\lambda) \Big) + \frac{\beta_1^3}{\beta_0^5} \left(\frac{\lambda(-12+42\lambda-64\lambda^2+25\lambda^3)}{36(1-\lambda)^4} \right. \\
& - \frac{(1-4\lambda+9\lambda^2)}{3(1-\lambda)^4} \ln(1-\lambda) - \frac{\lambda}{(1-\lambda)^4} \ln^2(1-\lambda) - \frac{1-4\lambda}{3(1-\lambda)^4} \ln^3(1-\lambda) \Big) \\
& + \left[\frac{\beta_2}{3\beta_0^2} \frac{(3+4\lambda-\lambda^2)\lambda^2}{(1-\lambda)^4} + \frac{\beta_1^2}{\beta_0^3} \left(- \frac{(3+4\lambda-\lambda^2)\lambda^2}{3(1-\lambda)^4} - \frac{2\lambda}{(1-\lambda)^4} \ln(1-\lambda) \right. \right. \\
& - \frac{1-4\lambda}{(1-\lambda)^4} \ln^2(1-\lambda) \Big) \Big] \ln \frac{Q^2}{\mu_R^2} + \frac{\beta_1}{\beta_0} \left[- \frac{\lambda}{(1-\lambda)^4} - \frac{1-4\lambda}{(1-\lambda)^4} \ln(1-\lambda) \right] \ln^2 \frac{Q^2}{\mu_R^2} \\
& + \frac{\beta_0}{3} \frac{\lambda^2(6-4\lambda+\lambda^2)}{(1-\lambda)^4} \ln^3 \frac{Q^2}{\mu_R^2} + \overline{B}^{(1)} \left(- \frac{\beta_3}{6\beta_0^2} \frac{(3-2\lambda)\lambda^2}{(1-\lambda)^3} + \frac{\beta_1\beta_2}{\beta_0^3} \left(\frac{(3-2\lambda)\lambda^2}{3(1-\lambda)^3} \right. \right. \\
& + \frac{\lambda}{(1-\lambda)^3} \ln(1-\lambda) \Big) + \frac{\beta_1^3}{\beta_0^4} \left(- \frac{(3-2\lambda)\lambda^2}{6(1-\lambda)^3} - \frac{\lambda}{(1-\lambda)^3} \ln(1-\lambda) - \frac{\ln^2(1-\lambda)}{2(1-\lambda)^3} \right. \\
& + \frac{\ln^3(1-\lambda)}{3(1-\lambda)^3} \Big) + \left[\frac{\beta_2}{\beta_0} \frac{\lambda}{(1-\lambda)^3} + \frac{\beta_1^2}{\beta_0^2} \left(- \frac{\lambda}{(1-\lambda)^3} - \frac{\ln(1-\lambda)}{(1-\lambda)^3} + \frac{\ln^2(1-\lambda)}{(1-\lambda)^3} \right) \right] \ln \frac{Q^2}{\mu_R^2} \\
& + \beta_1 \left[- \frac{\lambda(3-3\lambda+\lambda^2)}{2(1-\lambda)^3} + \frac{\ln(1-\lambda)}{(1-\lambda)^3} \right] \ln^2 \frac{Q^2}{\mu_R^2} + \beta_0^2 \frac{\lambda(3-3\lambda+\lambda^2)}{3(1-\lambda)^3} \ln^3 \frac{Q^2}{\mu_R^2} \Big) \\
& + A^{(1)} \left(\frac{\beta_2^2}{3\beta_0^4} \left(\frac{\lambda(-12+42\lambda-52\lambda^2+7\lambda^3)}{12(1-\lambda)^4} - \ln(1-\lambda) \right) \right. \\
& + \frac{\beta_4}{3\beta_0^3} \left(\frac{\lambda(12-42\lambda+40\lambda^2-13\lambda^3)}{12(1-\lambda)^4} + \ln(1-\lambda) \right) + \frac{\beta_1\beta_3}{6\beta_0^4} \left(- \frac{\lambda(2-5\lambda)}{3} \frac{(3-3\lambda+\lambda^2)}{(1-\lambda)^4} \right. \\
& - \frac{2-8\lambda+9\lambda^2-10\lambda^3+4\lambda^4}{(1-\lambda)^4} \ln(1-\lambda) \Big) + \frac{\beta_1^2\beta_2}{\beta_0^5} \left(\frac{\lambda(12-42\lambda+52\lambda^2+5\lambda^3)}{36(1-\lambda)^4} \right. \\
& - \frac{(-1+3\lambda-3\lambda^2+3\lambda^3)}{3(1-\lambda)^3} \ln(1-\lambda) - \frac{3\lambda^2}{2(1-\lambda)^4} \ln^2(1-\lambda) \Big) + \frac{\beta_1^4}{2\beta_0^6} \left(- \frac{\lambda^3(2+3\lambda)}{6(1-\lambda)^4} \right. \\
& + \frac{\lambda^2(-3+2\lambda-2\lambda^2)}{3(1-\lambda)^4} \ln(1-\lambda) - \frac{(1-3\lambda)\lambda}{(1-\lambda)^4} \ln^2(1-\lambda) - \frac{1-6\lambda}{3(1-\lambda)^4} \ln^3(1-\lambda) \\
& + \frac{1-4\lambda}{6(1-\lambda)^4} \ln^4(1-\lambda) \Big) + \left[- \frac{\beta_3}{6\beta_0^2} \frac{\lambda^2(-3-2\lambda+2\lambda^2)}{(1-\lambda)^4} - \frac{\beta_1\beta_2}{\beta_0^3} \left(\frac{2\lambda^3}{3(1-\lambda)^3} + \frac{3\lambda^2}{(1-\lambda)^4} \ln(1-\lambda) \right) \right. \\
& + \frac{\beta_1^3}{\beta_0^4} \left(- \frac{\lambda^2(3-2\lambda+2\lambda^2)}{6(1-\lambda)^4} - \frac{(1-3\lambda)\lambda}{(1-\lambda)^4} \ln(1-\lambda) - \frac{1-6\lambda}{2(1-\lambda)^4} \ln^2(1-\lambda) \right. \\
& + \frac{1-4\lambda}{3(1-\lambda)^4} \ln^3(1-\lambda) \Big) \Big] \ln \frac{Q^2}{\mu_R^2} + \left[- \frac{3\beta_2}{2\beta_0} \frac{\lambda^2}{(1-\lambda)^4} + \frac{\beta_1^2}{2\beta_0^2} \left(- \frac{(1-3\lambda)\lambda}{(1-\lambda)^4} - \frac{(1-6\lambda)}{(1-\lambda)^4} \ln(1-\lambda) \right. \right. \\
& + \frac{(1-4\lambda)}{(1-\lambda)^4} \ln^2(1-\lambda) \Big) \Big] \ln^2 \frac{Q^2}{\mu_R^2} + \frac{\beta_1}{3} \left[\frac{\lambda(2+6\lambda-4\lambda^2+\lambda^3)}{2(1-\lambda)^4} + \frac{1-4\lambda}{(1-\lambda)^4} \ln(1-\lambda) \right] \ln^3 \frac{Q^2}{\mu_R^2} \\
& - \frac{\beta_0^2}{12} \frac{(6-4\lambda+\lambda^2)\lambda^2}{(1-\lambda)^4} \ln^4 \frac{Q^2}{\mu_R^2} \Big), \tag{28}
\end{aligned}$$

where

$$\lambda = \frac{1}{\pi} \beta_0 \alpha_S(\mu_R^2) L, \tag{29}$$

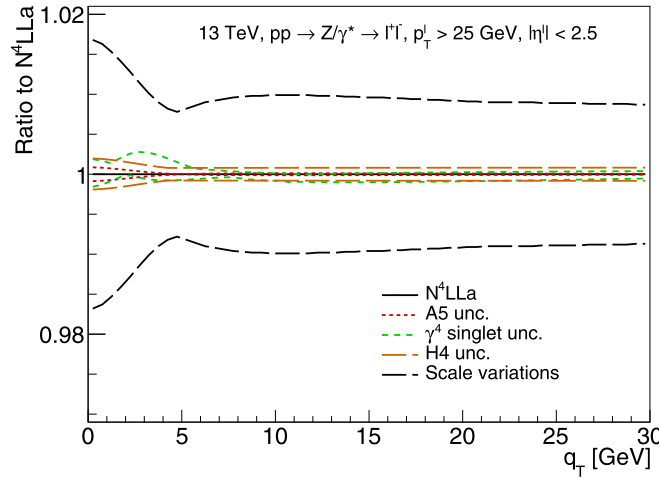


Fig. 5. Uncertainties arising from numerical approximations or incomplete knowledge of the perturbative coefficients at N^4LL+N^4LOa , compared to missing higher order uncertainties estimated with scale variations at this order.

$$\bar{B}^{(n)} = \tilde{B}^{(n)} + A^{(n)} \ln \frac{M^2}{Q^2} . \quad (30)$$

The $g^{(1)}$, $g^{(2)}$ and $g^{(3)}$ resummation functions can be found in Ref. [6]. The $g^{(4)}$ function can be found in Ref. [76] for the related case of direct transverse momentum space resummation. The explicit expression of the first five coefficients of the β function, can be found in the following references: β_0 , β_1 and β_2 in Refs. [77,78], β_3 in Ref. [79] and β_4 in [80].

At NLL+NLO we include the functions $g^{(1)}$, $g^{(2)}$ and $\mathcal{H}_V^{(1)}$, at NNLL+NNLO we also include the functions $g^{(3)}$ and $\mathcal{H}_V^{(2)}$ [70,81], at N^3LL+N^3LO the functions $g^{(4)}$ and $\mathcal{H}_V^{(3)}$ [82,83] and finally at N^4LL+N^3LO the function $g^{(5)}$ and $\mathcal{H}_V^{(4)}$.

In Fig. 5 we consider uncertainties in the numerical approximations of the N^4LL coefficients and arising from the incomplete knowledge of the N^4LO perturbative coefficients. The $B^{(4)}$ coefficient and the non-singlet four-loop splitting functions are known with good numerical approximation [84–88], the corresponding relative uncertainties on the q_T distribution are at the level of 10^{-6} or smaller, and considered negligible. The relative uncertainty due to the numerical approximations of $A^{(5)}$ [89–95] is also negligible for $q_T \gtrsim 4$ GeV and at the 10^{-3} level for $q_T \lesssim 4$ GeV. The numerical approximations the 4-loop singlet splitting functions [68,69] are the dominant uncertainties in the N^4LL approximation, and they amount to $1-3 \cdot 10^{-3}$ relative uncertainty. In order to estimate the size of the unknown $C^{(4)}$ coefficients [96] we perform a Levin transform of the corresponding perturbative series [66,67] to guess the value of the fourth term in these series, and assign to it a 100% uncertainty. This is equivalent to assuming that the Levin transform is able to estimate the sign and the order of magnitude of these unknown coefficients. The corresponding uncertainty is at the level of $1-2 \cdot 10^{-3}$, and affects mostly the overall normalization. The uncertainties in the N^4LL+N^4LO approximation are shown in Fig. 5, and found to be 5 to 10 times smaller compared to the missing higher order uncertainties estimated through scale variations.

References

- [1] S.D. Drell, Tung-Mow Yan, Massive lepton pair production in hadron-hadron collisions at high-energies, Phys. Rev. Lett. 25 (1970) 316–320. Erratum: Phys. Rev. Lett. 25 (1970) 902.
- [2] J.H. Christenson, G.S. Hicks, L.M. Lederman, P.J. Limon, B.G. Pope, E. Zavattini, Observation of massive muon pairs in hadron collisions, Phys. Rev. Lett. 25 (Nov 1970) 1523–1526.
- [3] Yuri L. Dokshitzer, Dmitri Diakonov, S.I. Troian, On the transverse momentum distribution of massive lepton pairs, Phys. Lett. B 79 (1978) 269–272.
- [4] G. Parisi, R. Petronzio, Small transverse momentum distributions in hard processes, Nucl. Phys. B 154 (1979) 427–440.
- [5] John C. Collins, Davison E. Soper, George F. Sterman, Transverse momentum distribution in Drell-Yan pair and W and Z boson production, Nucl. Phys. B 250 (1985) 199–224.
- [6] Giuseppe Bozzi, Stefano Catani, Daniel de Florian, Massimiliano Grazzini, Transverse-momentum resummation and the spectrum of the Higgs boson at the LHC, Nucl. Phys. B 737 (2006) 73–120.
- [7] Giuseppe Bozzi, Stefano Catani, Giancarlo Ferrera, Daniel de Florian, Massimiliano Grazzini, Transverse-momentum resummation: a perturbative study of Z production at the tevatron, Nucl. Phys. B 815 (2009) 174–197.
- [8] Giuseppe Bozzi, Stefano Catani, Giancarlo Ferrera, Daniel de Florian, Massimiliano Grazzini, Production of Drell-Yan lepton pairs in hadron collisions: transverse-momentum resummation at next-to-next-to-leading logarithmic accuracy, Phys. Lett. B 696 (2011) 207–213.
- [9] Stefano Catani, Massimiliano Grazzini, QCD transverse-momentum resummation in gluon fusion processes, Nucl. Phys. B 845 (2011) 297–323.
- [10] Thomas Becher, Matthias Neubert, Drell-Yan production at small q_T , transverse parton distributions and the collinear anomaly, Eur. Phys. J. C 71 (2011) 1665.
- [11] Thomas Becher, Matthias Neubert, Daniel Wilhelm, Electroweak gauge-boson production at small q_T : infrared safety from the collinear anomaly, J. High Energy Phys. 02 (2012) 124.
- [12] John Collins, Foundations of perturbative QCD, Camb. Monogr. Part. Phys. Nucl. Phys. Cosmol. 32 (2011) 1–624.
- [13] John C. Collins, Ted C. Rogers, Equality of two definitions for transverse momentum dependent parton distribution functions, Phys. Rev. D 87 (3) (2013) 034018.
- [14] Andrea Banfi, Mrinal Dasgupta, Simone Marzani, Lee Tomlinson, Predictions for Drell-Yan ϕ^* and Q_T observables at the LHC, Phys. Lett. B 715 (2012) 152–156.
- [15] Marco Guzzi, Pavel M. Nadolsky, Bowen Wang, Nonperturbative contributions to a resummed leptonic angular distribution in inclusive neutral vector boson production, Phys. Rev. D 90 (1) (2014) 014030.
- [16] John Collins, Ted Rogers, Understanding the large-distance behavior of transverse-momentum-dependent parton densities and the Collins-Soper evolution kernel, Phys. Rev. D 91 (7) (2015) 074020.
- [17] Stefano Catani, Daniel de Florian, Giancarlo Ferrera, Massimiliano Grazzini, Vector boson production at hadron colliders: transverse-momentum resummation and leptonic decay, J. High Energy Phys. 12 (2015) 047.
- [18] Markus A. Ebert, Frank J. Tackmann, Resummation of transverse momentum distributions in distribution space, J. High Energy Phys. 02 (2017) 110.
- [19] Francesco Coradeschi, Thomas Crigge, reSolve – A transverse momentum resummation tool, Comput. Phys. Commun. 238 (2019) 262–294.

- [20] Ignazio Scimemi, Alexey Vladimirov, Analysis of vector boson production within TMD factorization, *Eur. Phys. J. C* **78** (2) (2018) 89.
- [21] Wojciech Bizoń, Xuan Chen, Aude Gehrmann-De Ridder, Thomas Gehrmann, Nigel Glover, Alexander Huss, Pier Francesco Monni, Emanuele Re, Luca Rottoli, Paolo Torrielli, Fiducial distributions in Higgs and Drell-Yan production at $N^3LL+NNLO$, *J. High Energy Phys.* **12** (2018) 132.
- [22] Wojciech Bizon, Aude Gehrmann-De Ridder, Thomas Gehrmann, Nigel Glover, Alexander Huss, Pier Francesco Monni, Emanuele Re, Luca Rottoli, Duncan M. Walker, The transverse momentum spectrum of weak gauge bosons at $N^3LL+NNLO$, 2019.
- [23] Thomas Becher, Monika Hager, Event-Based Transverse Momentum Resummation, 2019.
- [24] Valerio Bertone, Ignazio Scimemi, Alexey Vladimirov, Extraction of unpolarized quark transverse momentum dependent parton distributions from Drell-Yan/Z-boson production, *J. High Energy Phys.* **06** (2019) 028.
- [25] Alessandro Bacchetta, Valerio Bertone, Chiara Bissolotti, Giuseppe Bozzi, Filippo Delcarro, Fulvio Piacenza, Marco Radici, Transverse-momentum-dependent parton distributions up to N^3LL from Drell-Yan data, *J. High Energy Phys.* **07** (2020) 117.
- [26] Markus A. Ebert, Johannes K.L. Michel, Iain W. Stewart, Frank J. Tackmann, Drell-Yan q_T Resummation of Fiducial Power Corrections at N^3LL , 2020.
- [27] Thomas Becher, Tobias Neumann, Fiducial q_T resummation of color-singlet processes at $N^3LL+NNLO$, 2020.
- [28] Emanuele Re, Luca Rottoli, Paolo Torrielli, Fiducial Higgs and Drell-Yan distributions at $N^3LL+NNLO$ with RadISH, 2021.
- [29] Simone Alioli, Christian W. Bauer, Alessandro Broggio, Alessandro Gavardi, Stefan Kallweit, Matthew A. Lim, Riccardo Nagar, Davide Napoletano, Luca Rottoli, Matching NNLO to parton shower using N^3LL colour-singlet transverse momentum resummation in Geneva, 2021.
- [30] Wan-Li Ju, Marek Schönherr, The q_T and $\Delta\phi$ spectra in W and Z production at the LHC at N^3LL+N^2LO , *J. High Energy Phys.* **10** (2021) 088.
- [31] Tobias Neumann, John Campbell, Fiducial Drell-Yan production at the LHC improved by transverse-momentum resummation at $N4LLp+N3LO$, *Phys. Rev. D* **107** (1) (2023) L011506.
- [32] Xuan Chen, Thomas Gehrmann, E.W.N. Glover, Alexander Huss, Pier Francesco Monni, Emanuele Re, Luca Rottoli, Paolo Torrielli, Third-order fiducial predictions for Drell-Yan production at the LHC, *Phys. Rev. Lett.* **128** (25) (2022) 252001.
- [33] Alessandro Bacchetta, Valerio Bertone, Chiara Bissolotti, Giuseppe Bozzi, Matteo Cerutti, Fulvio Piacenza, Marco Radici, Andrea Signori, Unpolarized transverse momentum distributions from a global fit of Drell-Yan and semi-inclusive deep-inelastic scattering data, *J. High Energy Phys.* **10** (2022) 127.
- [34] Duane A. Dicus, Scott S.D. Willenbrock, Radiative corrections to the ratio of Z and W boson production, *Phys. Rev. D* **34** (1986) 148.
- [35] P.J. Rijken, W.L. van Neerven, Heavy flavor contributions to the Drell-Yan cross-section, *Phys. Rev. D* **52** (1995) 149–161.
- [36] Long Chen, Michał Czakon, Marco Niggettiedt, The complete singlet contribution to the massless quark form factor at three loops in QCD, *J. High Energy Phys.* **12** (2021) 095.
- [37] R.N. Lee, A.V. Smirnov, V.A. Smirnov, Analytic results for massless three-loop form factors, *J. High Energy Phys.* **04** (2010) 020.
- [38] T. Gehrmann, E.W.N. Glover, T. Huber, N. Ikizlerli, C. Studerus, Calculation of the quark and gluon form factors to three loops in QCD, *J. High Energy Phys.* **06** (2010) 094.
- [39] Radja Boughezal, Christfried Focke, Xiaohui Liu, Frank Petriello, W -boson production in association with a jet at next-to-next-to-leading order in perturbative QCD, *Phys. Rev. Lett.* **115** (6) (2015) 062002.
- [40] A. Gehrmann-De Ridder, T. Gehrmann, E.W.N. Glover, A. Huss, T.A. Morgan, Precise QCD predictions for the production of a Z boson in association with a hadronic jet, *Phys. Rev. Lett.* **117** (2) (2016) 022001.
- [41] Radja Boughezal, John M. Campbell, R. Keith Ellis, Christfried Focke, Walter T. Giele, Xiaohui Liu, Frank Petriello, Z -boson production in association with a jet at next-to-next-to-leading order in perturbative QCD, *Phys. Rev. Lett.* **116** (15) (2016) 152001.
- [42] Radja Boughezal, Xiaohui Liu, Frank Petriello, W -boson plus jet differential distributions at NNLO in QCD, *Phys. Rev. D* **94** (11) (2016) 113009.
- [43] Radja Boughezal, Xiaohui Liu, Frank Petriello, Phenomenology of the Z -boson plus jet process at NNLO, *Phys. Rev. D* **94** (7) (2016) 074015.
- [44] Aude Gehrmann-De Ridder, T. Gehrmann, E.W.N. Glover, A. Huss, T.A. Morgan, The NNLO QCD corrections to Z boson production at large transverse momentum, *J. High Energy Phys.* **07** (2016) 133.
- [45] A. Gehrmann-De Ridder, T. Gehrmann, E.W.N. Glover, A. Huss, T.A. Morgan, NNLO QCD corrections for Drell-Yan p_T^Z and ϕ^* observables at the LHC, *J. High Energy Phys.* **11** (2016) 094. Erratum: *J. High Energy Phys.* **10** (2018) 126.
- [46] A. Gehrmann-De Ridder, T. Gehrmann, E.W.N. Glover, A. Huss, D.M. Walker, Next-to-next-to-leading-order QCD corrections to the transverse momentum distribution of weak gauge bosons, *Phys. Rev. Lett.* **120** (12) (2018) 122001.
- [47] Stefano Camarda, et al., DYTurbo: fast predictions for Drell-Yan processes, *Eur. Phys. J. C* **80** (3) (2020) 251. Erratum: *Eur. Phys. J. C* **80** (2020) 440.
- [48] Stefano Camarda, et al., DYTurbo.
- [49] Stefano Camarda, Leandro Cieri, Giancarlo Ferrera, Drell-Yan lepton-pair production: q_T resummation at N3LL accuracy and fiducial cross sections at N3LO, *Phys. Rev. D* **104** (11) (2021) L111503.
- [50] J. McGowan, T. Cridge, L.A. Harland-Lang, R.S. Thorne, Approximate N^3LO parton distribution functions with theoretical uncertainties: MSHT20aN 3LO PDFs, *Eur. Phys. J. C* **83** (3) (2023) 185. Erratum: *Eur. Phys. J. C* **83** (2023) 302.
- [51] John C. Collins, Davison E. Soper, Angular distribution of dileptons in high-energy hadron collisions, *Phys. Rev. D* **16** (1977) 2219.
- [52] John C. Collins, Davison E. Soper, Back-to-back jets: Fourier transform from B to K-transverse, *Nucl. Phys. B* **197** (1982) 446–476.
- [53] Stefano Catani, Michelangelo L. Mangano, Paolo Nason, Luca Trentadue, The resummation of soft gluons in hadronic collisions, *Nucl. Phys. B* **478** (1996) 273–310.
- [54] Eric Laenen, George F. Sterman, Werner Vogelsang, Higher order QCD corrections in prompt photon production, *Phys. Rev. Lett.* **84** (2000) 4296–4299.
- [55] Anna Kulesza, George F. Sterman, Werner Vogelsang, Joint resummation in electroweak boson production, *Phys. Rev. D* **66** (2002) 014011.
- [56] Andrea Signori, Alessandro Bacchetta, Marco Radici, Gunar Schnell, Investigations into the flavor dependence of partonic transverse momentum, *J. High Energy Phys.* **11** (2013) 194.
- [57] Luca Barze, Guido Montagna, Paolo Nason, Oreste Nicrosini, Fulvio Piccinini, Implementation of electroweak corrections in the POWHEG BOX: single W production, *J. High Energy Phys.* **04** (2012) 037.
- [58] Luca Barze, Guido Montagna, Paolo Nason, Oreste Nicrosini, Fulvio Piccinini, Alessandro Vicini, Neutral current Drell-Yan with combined QCD and electroweak corrections in the POWHEG BOX, *Eur. Phys. J. C* **73** (6) (2013) 2474.
- [59] S. Alioli, et al., Precision studies of observables in $pp \rightarrow W \rightarrow l\nu_l$ and $pp \rightarrow \gamma, Z \rightarrow l^+l^-$ processes at the LHC, *Eur. Phys. J. C* **77** (5) (2017) 280.
- [60] Leandro Cieri, Giancarlo Ferrera, German F.R. Sborlini, Combining QED and QCD transverse-momentum resummation for Z boson production at hadron colliders, *J. High Energy Phys.* **08** (2018) 165.
- [61] Andrea Autieri, Leandro Cieri, Giancarlo Ferrera, German F.R. Sborlini, Combining QED and QCD transverse-momentum resummation for W and Z boson production at hadron colliders, *J. High Energy Phys.* **07** (2023) 104.
- [62] Stefan Berge, Pavel M. Nadolsky, Fredrick I. Olness, Heavy-flavor effects in soft gluon resummation for electroweak boson production at hadron colliders, *Phys. Rev. D* **73** (2006) 013002.
- [63] Emanuele Bagnaschi, Fabio Maltoni, Alessandro Vicini, Marco Zaro, Lepton-pair production in association with a $b\bar{b}$ pair and the determination of the W boson mass, *J. High Energy Phys.* **07** (2018) 101.
- [64] Piotr Pietrulewicz, Daniel Samitz, Anne Spiering, Frank J. Tackmann, Factorization and resummation for massive quark effects in exclusive Drell-Yan, *J. High Energy Phys.* **08** (2017) 114.
- [65] Rhorry Gauld, A massive variable flavour number scheme for the Drell-Yan process, *SciPost Phys.* **12** (1) (2022) 024.
- [66] Andre David, Giampiero Passarino, How well can we guess theoretical uncertainties?, *Phys. Lett. B* **726** (2013) 266–272.
- [67] David Levin, Development of non-linear transformations for improving convergence of sequences, *Int. J. Comput. Math.* **3** (1972) 371–388.
- [68] S. Moch, B. Ruijl, T. Ueda, J.A.M. Vermaasen, A. Vogt, Low moments of the four-loop splitting functions in QCD, *Phys. Lett. B* **825** (2022) 136853.
- [69] G. Falcioni, F. Herzog, S. Moch, A. Vogt, Four-loop splitting functions in QCD – the quark-quark case, *Phys. Lett. B* **842** (2023) 137944.
- [70] Stefano Catani, Leandro Cieri, Daniel de Florian, Giancarlo Ferrera, Massimiliano Grazzini, Vector boson production at hadron colliders: hard-collinear coefficients at the NNLO, *Eur. Phys. J. C* **72** (2012) 2195.
- [71] Giuseppe Bozzi, Stefano Catani, Daniel de Florian, Massimiliano Grazzini, Higgs boson production at the LHC: transverse-momentum resummation and rapidity dependence, *Nucl. Phys. B* **791** (2008) 1–19.
- [72] G. Bozzi, S. Catani, D. de Florian, M. Grazzini, The $q(T)$ spectrum of the Higgs boson at the LHC in QCD perturbation theory, *Phys. Lett. B* **564** (2003) 65–72.

- [73] Stefano Catani, Daniel de Florian, Massimiliano Grazzini, Universality of nonleading logarithmic contributions in transverse momentum distributions, *Nucl. Phys. B* 596 (2001) 299–312.
- [74] Stefano Catani, Leandro Cieri, Daniel de Florian, Giancarlo Ferrera, Massimiliano Grazzini, Universality of transverse-momentum resummation and hard factors at the NNLO, *Nucl. Phys. B* 881 (2014) 414–443.
- [75] Stefano Catani, Giancarlo Ferrera, unpublished.
- [76] Wojciech Bizon, Pier Francesco Monni, Emanuele Re, Luca Rottoli, Paolo Torrielli, Momentum-space resummation for transverse observables and the Higgs p_\perp at $N^3LL+NNLO$, *J. High Energy Phys.* 02 (2018) 108.
- [77] O.V. Tarasov, A.A. Vladimirov, A.Yu. Zharkov, The Gell-Mann-low function of QCD in the three loop approximation, *Phys. Lett. B* 93 (1980) 429–432.
- [78] S.A. Larin, J.A.M. Vermaasen, The three loop QCD beta function and anomalous dimensions, *Phys. Lett. B* 303 (1993) 334–336.
- [79] T. van Ritbergen, J.A.M. Vermaasen, S.A. Larin, The four loop beta function in quantum chromodynamics, *Phys. Lett. B* 400 (1997) 379–384.
- [80] F. Herzog, B. Ruijl, T. Ueda, J.A.M. Vermaasen, A. Vogt, The five-loop beta function of Yang-Mills theory with fermions, *J. High Energy Phys.* 02 (2017) 090.
- [81] Thomas Gehrmann, Thomas Lubbert, Lin Li Yang, Transverse parton distribution functions at next-to-next-to-leading order: the quark-to-quark case, *Phys. Rev. Lett.* 109 (2012) 242003.
- [82] Ming-xing Luo, Tong-Zhi Yang, Hua Xing Zhu, Yu Jiao Zhu, Quark transverse parton distribution at the next-to-next-to-next-to-leading order, *Phys. Rev. Lett.* 124 (9) (2020) 092001.
- [83] Markus A. Ebert, Bernhard Mistlberger, Gherardo Vita, Transverse momentum dependent PDFs at N^3LO , *J. High Energy Phys.* 09 (2020) 146.
- [84] Goutam Das, Sven-Olaf Moch, Andreas Vogt, Soft corrections to inclusive deep-inelastic scattering at four loops and beyond, *J. High Energy Phys.* 03 (2020) 116.
- [85] Ian Moult, Hua Xing Zhu, Yu Jiao Zhu, The four loop QCD rapidity anomalous dimension, *J. High Energy Phys.* 08 (2022) 280.
- [86] Claude Duhr, Bernhard Mistlberger, Gherardo Vita, Four-loop rapidity anomalous dimension and event shapes to fourth logarithmic order, *Phys. Rev. Lett.* 129 (16) (2022) 162001.
- [87] Claude Duhr, Bernhard Mistlberger, Gherardo Vita, Soft integrals and soft anomalous dimensions at N^3LO and beyond, *J. High Energy Phys.* 09 (2022) 155.
- [88] S. Moch, B. Ruijl, T. Ueda, J.A.M. Vermaasen, A. Vogt, Four-loop non-singlet splitting functions in the planar limit and beyond, *J. High Energy Phys.* 10 (2017) 041.
- [89] F. Herzog, S. Moch, B. Ruijl, T. Ueda, J.A.M. Vermaasen, A. Vogt, Five-loop contributions to low-N non-singlet anomalous dimensions in QCD, *Phys. Lett. B* 790 (2019) 436–443.
- [90] Johannes M. Henn, Gregory P. Korchemsky, Bernhard Mistlberger, The full four-loop cusp anomalous dimension in $\mathcal{N} = 4$ super Yang-Mills and QCD, *J. High Energy Phys.* 04 (2020) 018.
- [91] Andreas von Manteuffel, Erik Panzer, Robert M. Schabinger, Cusp and collinear anomalous dimensions in four-loop QCD from form factors, *Phys. Rev. Lett.* 124 (16) (2020) 162001.
- [92] Ye Li, Hua Xing Zhu, Bootstrapping rapidity anomalous dimensions for transverse-momentum resummation, *Phys. Rev. Lett.* 118 (2) (2017) 022004.
- [93] Alexey A. Vladimirov, Correspondence between soft and rapidity anomalous dimensions, *Phys. Rev. Lett.* 118 (6) (2017) 062001.
- [94] S. Moch, J.A.M. Vermaasen, A. Vogt, The three loop splitting functions in QCD: the nonsinglet case, *Nucl. Phys. B* 688 (2004) 101–134.
- [95] Ye Li, Andreas von Manteuffel, Robert M. Schabinger, Hua Xing Zhu, Soft-virtual corrections to Higgs production at N^3LO , *Phys. Rev. D* 91 (2015) 036008.
- [96] Roman N. Lee, Andreas von Manteuffel, Robert M. Schabinger, Alexander V. Smirnov, Vladimir A. Smirnov, Matthias Steinhauser, Quark and gluon form factors in four-loop QCD, *Phys. Rev. Lett.* 128 (21) (2022) 212002.